Use of 3000 Bragg grating strain sensors distributed on four eight-meter optical fibers during static load tests of a composite structure

Brooks A. Childers [a], Mark E. Froggatt [a], Sidney G. Allison [b], Thomas C. Moore, Sr. [b], David A. Hare [b], Christopher F. Batten [c], Dawn C. Jegley [b]

[a]Luna Innovations, Blacksburg, VA, 24062
[b]NASA Langley Research Center, Hampton, VA, 23681
[c]Modern Machine & Tool Company, Newport News, VA, 23606

ABSTRACT

This paper describes the use of a fiber optic system to measure strain at thousands of locations along optical fibers where weakly reflecting Bragg gratings have been photoetched. The optical fibers were applied to an advanced composite transport wing along with conventional foil strain gages. A comparison of the fiber optic and foil gage systems used for this test will be presented including: a brief description of both strain data systems; a discussion of the process used for installation of the optical fiber; comparative data from the composite wing test; the processes used for the location and display of the high density fiber optic data. Calibration data demonstrating the potential accuracy of the fiber optic system will also be presented. The opportunities for industrial and commercial applications will be discussed. The fiber optic technique is shown to be a valuable augmentation to foil strain gages providing insight to structural behavior previously requiring reliance on modeling.

Keywords: Fiber optic sensing, optical frequency domain reflectometry, Bragg gratings

1. INTRODUCTION

Optical reflectometry techniques are useful for characterizing both long and short lengths of optical fiber. These techniques have been demonstrated in the time, coherence, and frequency domains.[1] Optical time domain reflectometry (OTDR) is useful for long links (kilometers) and is the principal instrument for characterization of optical fiber links in the telecommunications industry. These instruments are used to locate losses due to splices, connectors, and fiber bends. However, the spatial resolution of OTDR is limited to about 5cm. Both coherence and frequency domain techniques (OCDR and OFDR respectively) were developed for use on shorter links (< 1 meter), primarily to investigate the small spatial scale scattering properties of waveguides. Both are capable of resolutions on the order of 10 microns and were found to be useful for locating reflective surfaces when diagnosing multi-element fiberoptic components, e.g. lasers, detectors, isolators, etc. OCDR has traditionally been the commercial winner over OFDR in this area. With the recent availability of widely tunable mode-hop free lasers, OFDR is poised to become the technique of choice with a broader application potential than OCDR. One of those applications for the demodulation of highly distributed fiber Bragg grating (FBG) sensors is the subject of this paper. Specifically the use of OFDR to measure strain at 3000 locations during the static load testing of an advanced composite aerospace structure is discussed.

A static load test of a stitched composite semi-span wing was recently conducted at NASA's Langley Research Center (LaRC).[2] The test was the culmination of a ten year program started under the Advanced Composites Technology Program. The goal of the program was to reduce cost and weight of composite primary structure while improving damage tolerance and performance. The wing was designed to represent the inboard 40 feet of the wing of a generic 200-passenger commercial transport. The wing is made from graphite-epoxy and has Kevlar™ stitches through the thickness. The stitching improves damage tolerance by reducing the potential for delamination and therefore limiting and containing damage. It also reduces or eliminates the need for mechanical fasteners, thereby reducing the part count, the labor hours, and generally reducing the fabrication costs. The stitched wing cover panels contained no fasteners. Eliminating fasteners has the added benefit of eliminating holes where cracks can initiate, thereby reducing inspection time and improving safety.

A total of 466 conventional foil strain gages were used in the test. These were located at key sites throughout the wing as predicted by analysis. Two areas where it was determined that densely distributed strain measurements could prove useful were sites where damage was intentionally induced, and sites predicted by analysis to sustain the largest strains. The OFDR technique, which has been under development in the Non-Destructive Evaluation Sciences Branch at LaRC over the last few

years, had recently advanced to the point where high density measurements were possible.[3,4] Four eight meter long singlemode optical fibers, each containing 800 Bragg grating sensors, were bonded to the wing in an attempt to obtain data at critical and non-critical locations. This measurement was an ad hoc addition to the overall test program, and while moderately successful, the error sources and sensor calibration needs to be more fully understood. Consequently, while the test data presented will demonstrate the potential of the technique, it will not be used to interpret results from the stitched composite semi-span wing test.

After a brief discussion of how OFDR can distinguish between the hundreds of FBG sensors on the fibers, a comparison of the use of highly distributed FBGs and foil strain gages for this test will be given followed by a conclusion containing some commentary on future use and development of the system.

2. OPTICAL FREQUENCY DOMAIN REFLECTOMETRY (OFDR)

Optical frequency domain reflectometry can be used to measure the wavelength of light reflected from literally thousands of low reflectivity Bragg gratings distributed along singlemode fibers. The distribution of light wavelengths (or spectrum) reflected from an FBG is influenced by the temperature and strain state of the device to which it is attached. Consequently, FBG's attached to a structure can be used to measure either its temperature or strain. FBG's can also be used for a wider variety of sensing applications depending only upon the ingenuity of the user, e.g. corrosion, hazardous gas concentration, pressure, etc.[5]

The light spectrum reflected by a FBG is a fundamental property of the refractive index modulation laser etched into the core of the fiber during manufacture. The mean value of the spectrum is governed by the mean modulation period. If FBGs are attached to a material or structure early in it's life cycle, they can monitor the residual stresses induced by subsequent material processing as well as the strain history over the life of the structure. This information can provide insight into the ultimate performance capability of a structure. Since optical fiber is made of glass which is very strong in both tension and compression, the range of strains that can be measured is sufficient for most applications. It has also been shown that the pattern etching process does not effect the strength of the optical fiber.[6,7]

The coupled mode equations give a theoretical foundation for the spectrum of a Bragg grating with arbitrary reflectivity.[3] However, for the low reflectivity FBG arrays useful in this work, the following approximate description of the demodulation of their individual spectra is sufficient.

The basic OFDR consists of a wavelength tunable laser, three 2-by-2 couplers, two photodiode detectors, an FBG array, and an in-fiber interferometer. This arrangement is shown in Figure 1.

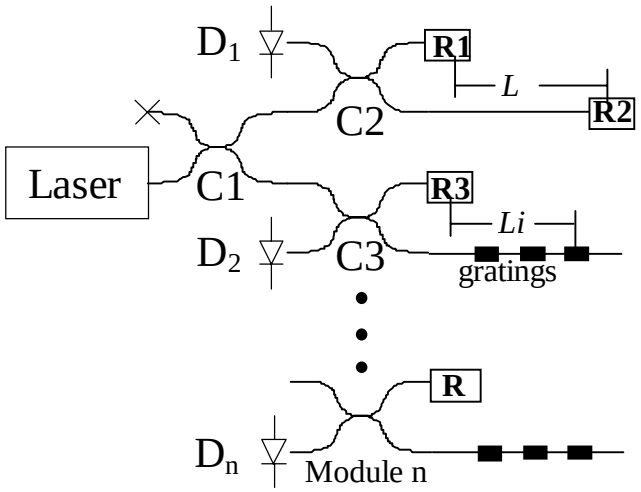

Figure 1. Sketch of the OFDR layout. Items C1, C2, and C3 are fiber couplers. The items marked R1-3 are broadband reflectors. The "X" is used to represent termination of an unused optical path. Additional sensing modules are easily added as shown.

The laser light is split by coupler 1 and travels to couplers 2 and 3. Coupler 2 is used to form an in-fiber interferometer with the light reflected from R1 and R2, detected at D_1. This interferometer has an optical path length difference of $2nL$ where n is the effective index of the fiber and L is the path difference of the two paths through the interferometer. Coupler 3 is used to form a sequence of overlapping interferometers. These interferometers are formed with the light reflected from R3 and each grating, detected at D_2. The system is easily extendable by adding sensor modules as indicated in the Figure 1.

The OFDR signals are driven by the wavelength tuning of the laser. As the laser is tuned, the signal at D_1 is given by

$$D_1 = \cos(k2nL). \quad (1)$$

The frequency of this signal is proportional to L, the interferometer path length difference. The constant k is the wavenumber of the light and is related to the light's wavelength, λ, by

$$k = \frac{2\pi}{\lambda}. \quad (2)$$

The interferometer is shown to cycle once for a wavenumber change, Δk ,of

$$\Delta k = \frac{\pi}{nL}. \quad (3)$$

This is a constant and shows that the interferometer cycles linearly as a function of wavenumber. The positive going zero crossing of the signal on D_1 is used to trigger the sampling of the signal on D_2. This guarantees that the signal at D_2 is sampled at the constant wavenumber interval given by Equation (3).

A multitude of signals are present at D_2, each similar to the signal at D_1 since they are also interferometer outputs. However the response of each interferometer is limited to the narrow wavelength range, or spectrum, over which its grating reflects. In other words, the individual interferometers can only produce an output signal when their gratings are reflecting light. The signal at D_2 is then given by the sum of interferometer responses, each of which is limited by the spectrum of its grating. So the signal at D_2 can be written as

$$D_2 = \sum_i R_i \cos(k2nL_i). \quad (4)$$

Where R_i is the spectrum of the *i*'th grating and L_i is the path length difference of the corresponding i'th interferometer. This equation shows the important result that the spectrum of each grating is modulated by a signal with a unique frequency which is governed by the grating's position, L_i, in the fiber. By bandpass filtering around a specific frequency (location) via fast Fourier transformation, the spectrum of each grating can be independently measured and strain or temperature inferred.

The graphs shown in Figure 2 are examples of data acquired with the fiber optic system. This data was acquired on a fiber with FBGs similar in manufacture to that used in the test except that the FBGs are spaced 2.54 cm apart, and the gratings were limited to a shorter 3 meter section at the end of a 6.5 meter fiber. The exact configuration of a sensing fiber is somewhat inconsequential to the data processing and can be either tailored to a particular test, or, the FBGs can simply be spaced together as closely as possible for maximum coverage. Figure 2a shows the magnitude of a complete set of raw data after initial Fourier transformation. Figure 2b shows an expanded view of a 20 cm subset of this data clearly showing the distinct FBG profiles in the fiber. Figure 2c shows the spectrum of a single FBG obtained by inverse Fourier transformation of an even smaller subset containing only one grating. Some figure of merit for determining the central value of the spectral peak is used to determine the grating's reflected wavenumber. The temperature independent equation governing the use of FBGs for strain sensing is given approximately by

$$\frac{\Delta k}{k} = K\varepsilon \quad (5)$$

where Δk is the strain induced wavenumber shift of a grating, k is the wavenumber of the laser, ε is the strain seen by the FBG, and K is a constant of proportionality typically given between 0.7 and 0.8. Determination of the proportionality constant is similar to determining the gage factor for a resistive strain gage.

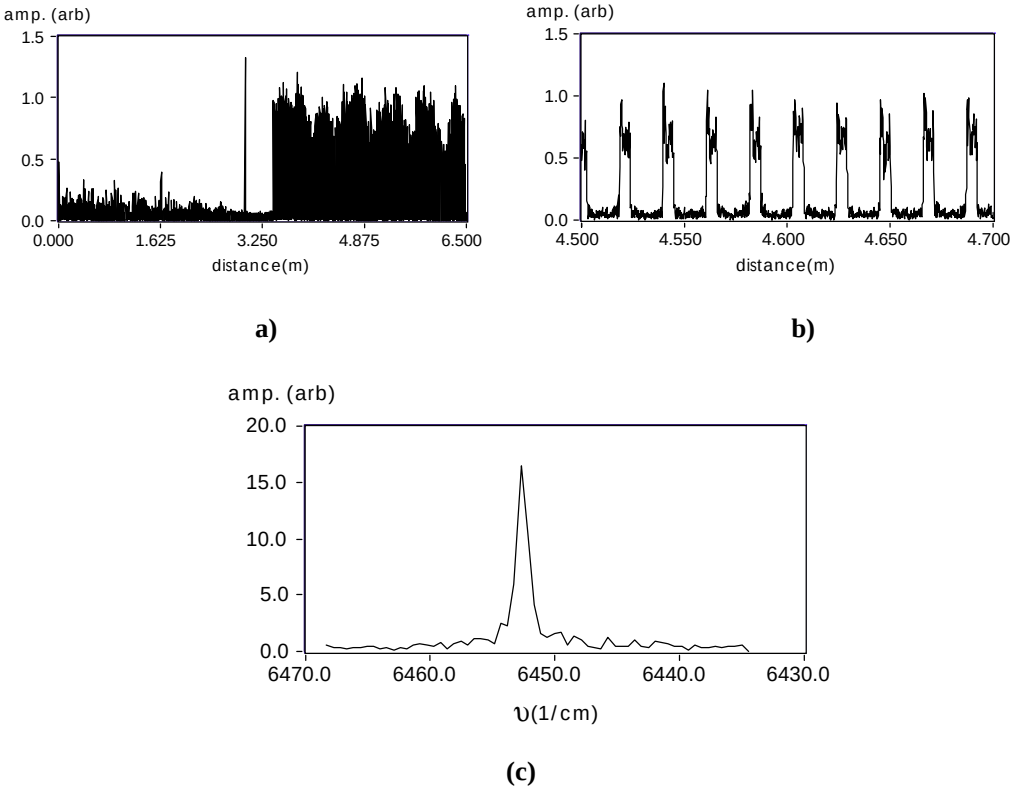

Figure 2. Typical data from the OFDR; a) reflected amplitude, b) close-up of gratings, c) recovered grating spectrum.

To determine a strain value, the initial wavenumber of a grating is acquired prior to test and then subtracted from the wavenumbers obtained during the test. The differences are Δk values used in Equation 5 to recover strain.

3. SYSTEM DESCRIPTIONS

3.1 FOIL STRAIN GAGE SYSTEM

The foil gage instrumentation was composed of a commercial 512 channel scanning analog-to-digital converter utilizing transducer dependent signal conditioning electronics as needed.[8] Data was acquired at 1 Hz and transferred to a real-time computer through a 16-bit parallel interface.[9] This computer utilizes a deterministic real-time operating system that asynchronously receives and services interrupt requests from the analog-to-digital converter insuring that all data is securely archived. The computer was programmed to provide six real-time x-y plots and printing of screen dumps during the course of testing. Proper attention to data security and real-time data assessment is critical for large scale structural testing to ultimate failure loads.

A total of 466 resistive strain gages were used in the test. These gages were added at several stages in the life of the test article. The following description pertains only to a particular set of 182 gages used in the test. Limiting the discussion to these gages will simplify the description of the installation process. Note, however, that these gages and the installation procedures used are considered typical for strain-gaging composite test articles for room temperature testing and provide a reasonable choice for comparison to the fiber installation. The encapsulated foil gages used were single element type CEA-

06-187UW-350 and three-element type CEA-06-125UR-350.[10] The gages were installed according to Application Class III, Installation Type 1 instructions found in Reference 11. The adhesive used for bonding the gages was M-BOND 200.[10] This adhesive is a widely-used cyanoacrylate strain-gaging adhesive which requires only "thumb pressure" at room temperature for about two minutes to set. Each gage required at least three wires to be routed to the data acquisition system through a large terminal block. These wires were also secured to the structure at points along their path to the terminal block using strips of aluminum tape and "ty-raps" to provide a neat installation. The estimated material and labor costs for the installation of the 182 gages is $3,000 and $7,000 respectively. Figure 3 shows photos of the conventional gage cable bundles and gage installations on the underside of the wing.

a) **b)**

Figure 3. a) Photo showing the cabling required to connect the conventional foil gages to the ADC hardware b) Photo showing large grey connector block below the composite wing. Five oval access panel cutouts are visible running along the bottom center of the wing. The large hydraulic actuators in the foreground are two of the nine actuators used to apply the test loads.

3.2 DISTRIBUTED FIBER OPTIC SYSTEM

The fiber optic instrumentation was composed of a laser diode, a four channel optical network, detectors, and a 900 MHz PC class desktop computer. The computer had commercial analog-to-digital conversion and GPIB bus cards installed along with their drivers and programming environment software.[12] The laser diode was a continuously tunable, mode-hop free, external cavity design commonly used in telecommunication test and measurement.[13] The laser was tuned in a 12 nm range centered about 1550 nm. The total laser power was approximately 5mW with approximately 1.0 mW transmitted to each channel. A photo of the fiber optic instrumentation is shown in Figure 4.

The raw data for all 3000 FBGs was acquired every 15 seconds. The laser scan accounted for about two seconds while writing the data to disk took about 13 seconds. The amount of raw data acquired is not governed by the number of FBGs in the fibers as might be expected, but by a combination of the length of the sensing fiber and the strain range to be covered. For this test an eight meter fiber and 12nm tuning range resulted in about 1 million points per laser scan. Data from the four fibers was acquired simultaneously and stored in four arrays of real numbers, each number occupying four bytes of storage for a total of 16 Mbytes. The raw data was processed after the test requiring another 30 seconds per scan with the bulk of the time required for intermediate reading and writing of data to and from storage. The ultimate result for each scan is simply a single strain value per FBG per laser scan.

The 9/125 micron core/cladding high numerical aperture sensing fiber was manufactured at LaRC on a research class fiber optic draw tower. The FBGs were etched into the fiber core with a 246nm UV laser using a typical two beam interferometer. The FBG locations were automatically marked with a pair of felt tip ink pens as the fiber was drawn. The coating was a 20 micron polyimide applied in two 10 micron layers. The FBGs were written in 8 meter sections with 1 cm spacing resulting in

800 FBGs per fiber. Each channel of the system was used to measure the 800 strain values on one 8 meter section. Figure 5 shows a photo of the sensing fiber next to a conventional foil gage.

Figure 4. A photo of the optical frequency domain reflectometer on top of a computer cart in place for the test. The black box on top contained the optical network, the white rack mount unit below the optical network is the tunable laser. Seen lying on the optical network and mounted beside the laser are battery powered commercial detectors. Note the leads to the four sensing fibers taped to the wall for comparison with the bundle of wire leads required for the conventional system shown in Figure 3a.

The installation of the fiber was performed in the following manner. First the location of a fiber is determined in a similar manner as for conventional gage applications using scales and transits. To simplify the process for such a large number of gages, the fiber was laid out in straight lines and simple arcs. Only the locations of the transition points between straight and curved sections, along with two other points in the arc regions are measured. This data is used for fitting of straight lines and cubic curves through the measured points. The location of the FBGs in between the measured points are estimated by interpolation of the known grating spacing along the computed fiber path.

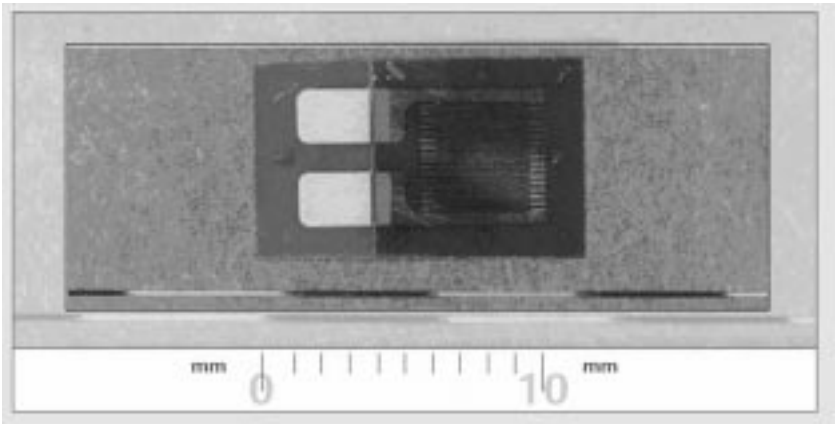

Figure 5. A side-by-side comparison of Bragg grating sensing fiber array and a conventional foil gage. The black ink marks on the fiber indicate the nominal locations and lengths of the fiber Bragg gratings.

The fiber path is then cleaned using a surface degreaser and ethyl alcohol, sanded, and then cleaned again. The fiber is then placed in the pre-determined locations using small pieces of polyimide tape to hold it in place. Next, the cement is brushed on

over the fiber so that the brush contacts the fiber and the surface that it is being bonded to. The cement draws the fiber close to the surface and capillary action carries the cement under the entire length of the fiber. The bond line is approximately .008" thick and completely encapsulates the fiber which provides mechanical protection.

After the cement cured overnight, the polyimide tape was removed and cement was applied to these areas and allowed to cure overnight. This procedure was followed for each of four fibers and took approximately fifty man-hours to accomplish with one technician working on the project except when two technicians were required to facilitate routing the fiber under difficult circumstances e.g. when the application was to the bottom surface of the wing. After the installation, the fiber was nearly invisible on the wing. The four fiber leads to the sensing fibers were attached to the wing at various points along their path to provide a neat installation. This was undertaken in a manner similar to that for conventional wire leads while care was taken not to induce bend losses in the leads.

Two types of cement were used to bond the fiber.[10] The cement initially chosen used was AE-10. When it was observed during the first application that it did not wet the ink marks indicating the FBG locations as well as it did the bare fiber, GA-2 was tried. The GA-2 had the same general reaction to the ink marks, but its wetting characteristics were determined the better of the two cements for this application and it was used for the remaining three fiber installations.

4. CALIBRATION AND TEST DATA COMPARISON

A direct comparison between the two strain measurement systems used for this test is problematic due to the large differences in the requirements of the two systems. The foil gage system was required to be a high reliability system providing both test data integrity and real time test monitoring for one-of-a-kind tests. The fiber system, although a second generation field deployable instrument, was assembled from lab equipment and not designed for real time data acquisition or high reliability.

One of the obvious benefits of the fiber optic system is the potential savings in installation cost per gage over conventional foil gages when the number of gages is high. Again, the most meaningful comparison would involve equal performance and reliability requirements for both gages, which was not the case for this test. Matching the performance and reliability of foil gages with FBGs will require significantly more engineering effort. In any case, these potential cost savings will be discussed along with the added benefit of high sensor density.

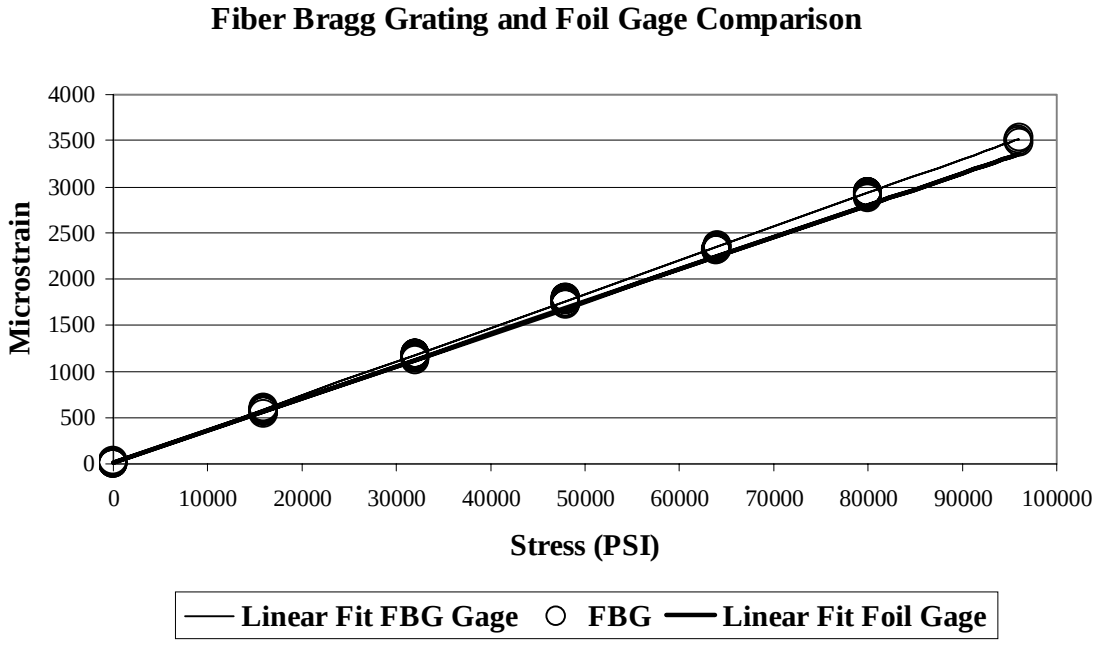

Figure 6. Comparison of a FBG and a foil strain gage in a lab calibration test.

A comparison of strain measured with the FBGs as described above with a conventional foil gage system in a calibration facility is given in Figure 6. The values for *K* assumed in the FBG measurements is 0.75. The circles show the repeatability

of the FBG measurements made through four load cycles and the linear fit through these data points shows a slightly higher slope than the foil gage. The slope error is due to the assumed value of K=0.75, which can be determined from data obtained in calibration tests such as these. Although a comprehensive calibration program for the FBGs has not been undertaken, the data shown in Figure 6 is typical and demonstrates the clear potential for FBGs as strain transducers.

Comparison of foil and FBG data from the stitched composite semi-span wing test is shown in Figure 7. This figure shows the strain vs load curve for four FBGs with the four nearest foil gages. These foil and FBG gages were spaced approximately 12 mm apart and oriented to measure the same strain component. The data demonstrates both the average accuracy of the FBG data and the variance of the FBG data. The value of K was again assumed to be 0.75 for this test. Some possible sources for both the apparent FBG inaccuracies and their large deviations compared to the foil gages include polarization effects such as inherent birefringence of the fiber, real non-uniform strain distributions along the FBG length, and real differences in the strain field between the foil and FBG gages.

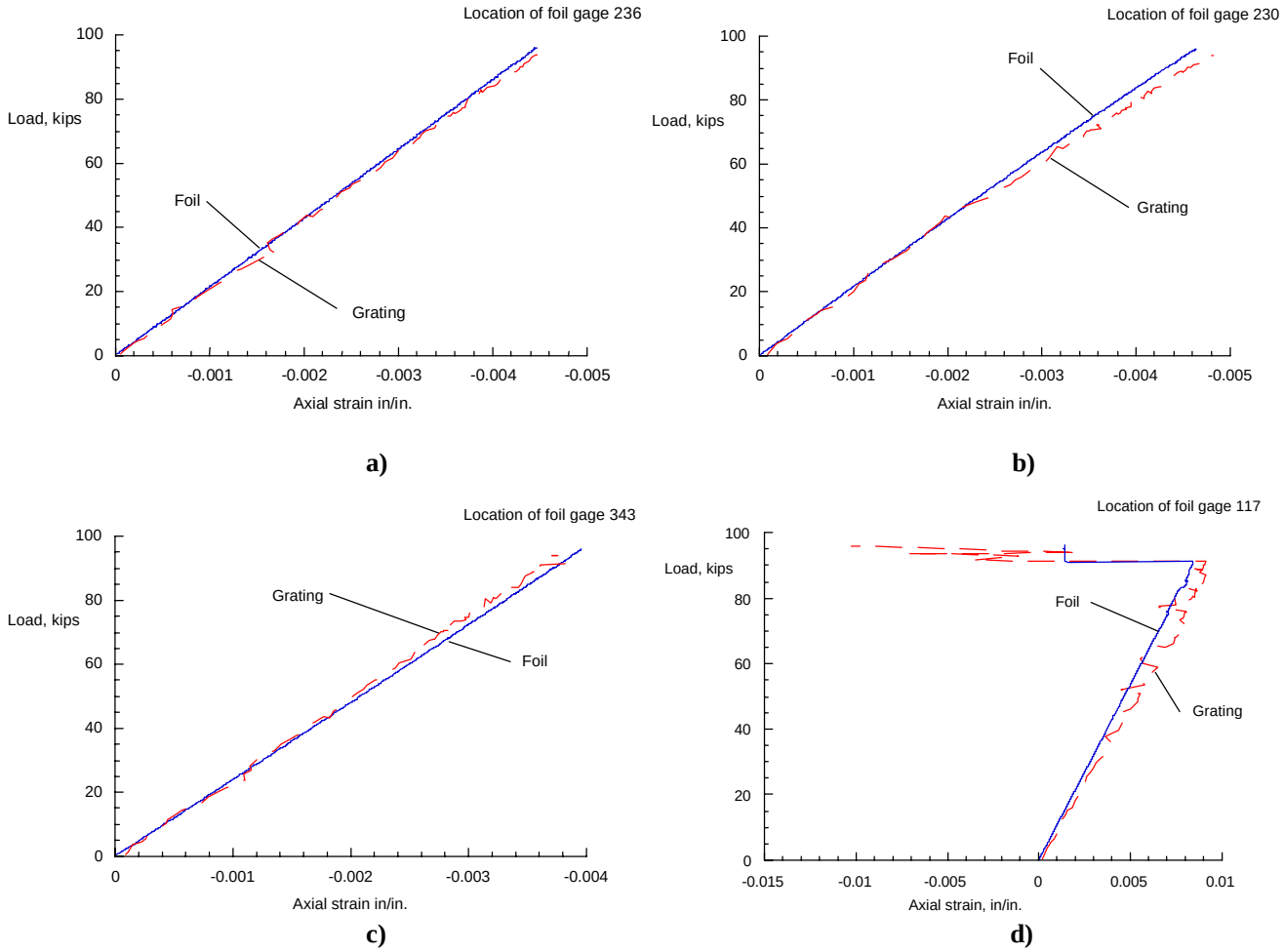

Figure 7. a)-d) Direct comparison of the data obtained during the final test to failure. The data in d) is the location of the highest strain levels and the location of one of the failure initiation points.

5. DISCUSSION

As mentioned above, an important feature of the highly distributed FBG approach is the much larger number of measurements that can be made for the same installation cost. These savings are realized through the reduction in labor involved in attaching the gages and then subsequent attachment and routing of lead wires. In order to use FBGs to completely replace the foil gages used in this test, many more fibers would need to be used to cover all of the features of the structure, in this case stringers, spars, etc. However, concurrent with the increased number of fibers is the large increase in the number of

measurements. The system is easily scalable and the system used in the test described does not represent a limit on the number of fibers or sensors that could be utilized.

Figure 8 shows the strain values of all 3000 FBGs on the four fibers just prior to the wing failure. Note that the fiber of Figure 8b broke shortly after installation near FBG 600 yielding about 3000 total FBG measurements instead of 3200. The fiber in 8a was routed around the perimeter of the access panel cutouts visible in the bottom of the wing in Figure 3b. The fibers in Figures 8b and 8c were placed in zig-zag patterns on the bottom and top of the wing respectively, near the trailing edge. The fiber in Figure 8d was placed straight along the main spar on the top of the wing.

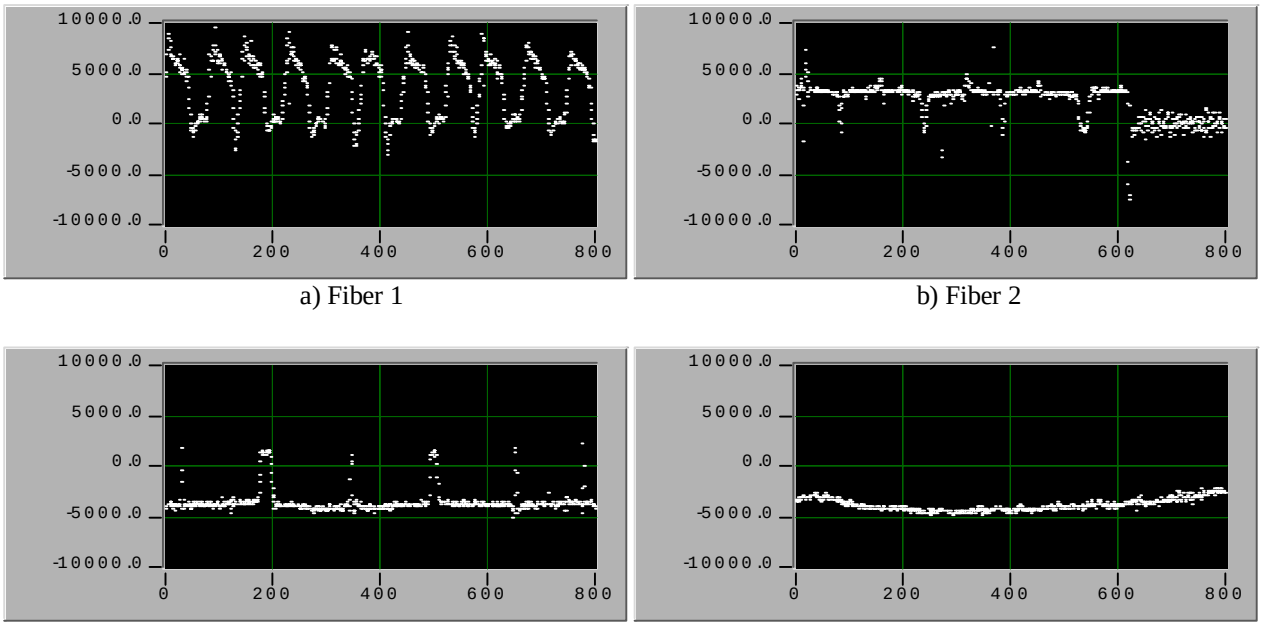

a) Fiber 1 b) Fiber 2

c) Fiber 3 d) Fiber 4

Figure 8. Microstrain vs FBG location in cm of the four FBG arrays attached to the composite wing just prior to failure.

Another important benefit derived from the high density of measurements is the ability to visualize strain contours on a structure. The graph in Figure 9 is a representation of a strain contour around the access panel cutouts in the bottom of the wing.

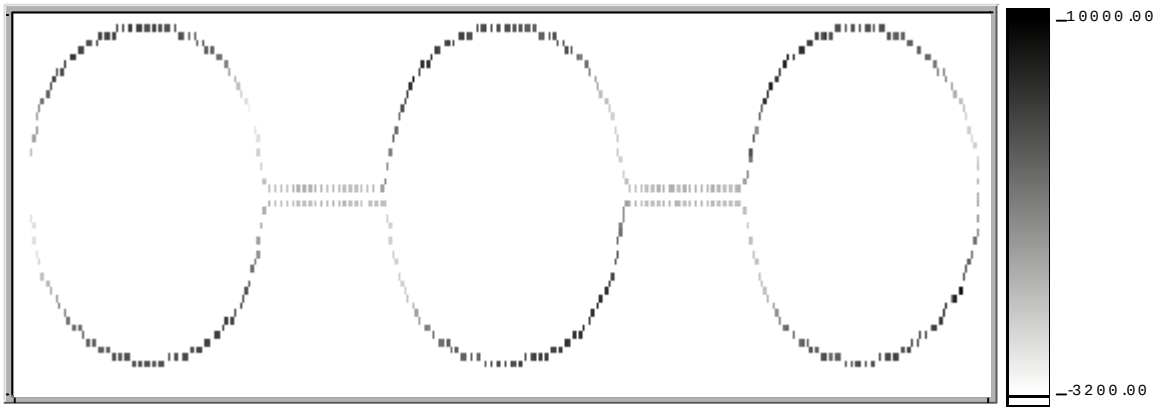

Figure 9. Gray scale representation of strain values from the fiber of Figure 8a overlayed on a two dimensional graphic representation of the fiber's layout on the wing. The gray scale is in microstrain from 10000 (black, tensile) to -3200 (white, compressive).

This type of data visualization is useful to further promote the test engineer's understanding of how the structure is behaving. It also hints at the possibility for a complete mapping of a the strain field of a structure. This could be accomplished by laying out the FBGs in a regular grid pattern. Although similar data is also available with full field imaging techniques such as photoelasticity, speckle photography, moire interferomerty or shearography, the fiber optic data is subject to much less interpretation, provides a greater range of application, and does not require optical access to the structure.

The location of conventional strain gages is a difficult engineering task requiring complex modeling of the structure in order to properly locate gauges where the maximum strains are anticipated or where phenomena of interest are occurring. The use of highly distributed FBGs can relax this procedure by allowing the entire structure, or at least large sections of the structure, to be completely covered with measurements. With this area coverage, the criticality of the placement of an individual strain gage is greatly diminished.

6. CONCLUSION

The use of an optical frequency domain reflectometer for readout of strain measured by 3000 fiber Bragg gratings distributed on four eight-meter optical fibers attached to a composite wing structure is described. This system is compared to the conventional foil gage system used for primary data acquisition during the test. Although an accurate cost comparison between the fiber and foil gage systems is not possible due to the different requirements placed on the two systems, the fiber system demonstrates a potential for savings in the labor required for gage and lead wire installation. The large numbers of gages possible with the fiber system may allow for complete coverage of areas of interest for some tests, relaxing the requirement for detailed modeling prior to testing for critical gage placement. Also by using large numbers of gages, strain contours and two dimensional strain field maps may be generated which will be valuable for interpretation of test results. Comprehensive calibration of the system remains to be accomplished although initial tests on calibration coupons demonstrates repeatable linear behavior of the FBG's at moderate strain levels. The sources of the large deviations in the FBG data for the composite wing test need to be determined through subsequent lab work and remedied by system modification and/or improved FBG application procedures.

7. REFERENCES

1. Derickson, Dennis, Ed. *Fiber Optic Test and Measurement*, Prentice Hall, Upper Saddle River, NJ, 1998.
2. Jegley, D. C., and Bush, H. G., "Structural Testing of a Stitched/Resin Film Infused Graphite-Epoxy Wing Box," to be published as NASA LaRC Technical Memorandum, 2001-xxxx.
3. Mark Froggatt, "Distributed measurement of the complex modulation of a photoinduced Bragg grating in an optical fiber", Appl. Opt. Vol. 35, No. 25, 1 Sept 1996, pp 5162-5164.
4. Mark Froggatt and Jason Moore, "Distributed measurement of static strain in an optical fiber with multiple Bragg gratings at nominally equal wavelengths", Appl. Opt. Vol. 37, No. 10, 1 April 1998.
5. Kersey, Alan D., Davis, Michael A., Patrick, Heather J., LeBlanc, Michel, Koo, K. P., Askins, C. G., Putnam, M. A., Friebele, E. Joseph, "Fiber Grating Sensors", J. of Lightwave Tech., 15(8), 8 August 1997.
6. Askins, C. G., Putnam, M. A., Patrick, H. J. and Friebele, E. J., "Fibre strength unaffected by on-line writing of single-pulse Bragg gratings", Elec. Lett. 33(15), 17 July 1997.
7. Hagemann, V., Trutzel, M. N., Staudigel, L., Rothhardt, M., Muller, H. R. and Krumpholz, O., "Mechanical resistance of draw-tower-Bragg-grating sensors", Elec. Lett., 34(2), 22 January 1998.
8. Neff Instrument Corporation, 700 Myrtle Avenue, Monrovia, CA, 91016.
9. MODCOMP, Inc., 1650 West McNab Road, Ft. Lauderdale, FL 33309-1088
10. Measurements Group Inc., P.O. Box 27777, Raleigh, NC 27611.
11. Moore, Thomas C., Sr., "Recommended Strain Gage Application Procedures for Various Langley Research Center Balances and Test Articles", NASA Technical Memorandum 110327, March 1997.
12. National Instruments Corporation , 11500 N Mopac Expwy, Austin, TX 78759-3504
13. New Focus, Inc. , 5215 Hellyer Ave., Suite 100, San Jose, CA 95138-1001

The use of trademarks or names of manufacturers in the report is for accurate reporting and does not constitute an official endorsement, either expressed or implied, of such products or manufactures by the National Aeronautics and Space Administration.